

Derivation of a Three-Dimensional Pharmacophore Model of Substance P Antagonists Bound to the Neurokinin-1 Receptor

Yasuo Takeuchi,[†] E. F. Berkley Shands,[‡] Denise D. Beusen,^{†,§} and Garland R. Marshall^{*,†}

Center for Molecular Design and Department of Computer Science, Washington University, St. Louis, Missouri 63110-1012

Received January 9, 1997

Constrained systematic search was used in an exhaustive conformational analysis of a structurally diverse set of substance P (SP) antagonists to identify a unique hypothesis for their bound conformation at the neurokinin-1 receptor. In this conformation, two aromatic groups essential for high affinity adopt a perpendicular or edge-on arrangement. This pharmacophore hypothesis for the receptor-bound conformation was used in a comparative molecular field analysis (CoMFA) of an expanded set of SP antagonists, and the predictive ability of the resulting three-dimensional quantitative structure–activity relationship (3D-QSAR) was evaluated against a test set of SP antagonists different from those in the training set. This CoMFA model based on the Constrained Search alignment yielded significant cross-validated, conventional, and predictive r^2 values equal to 0.70, 0.93, and 0.82, respectively. For comparison, the SP antagonists were forced into an alternative poorer alignment in which the two aromatic rings were parallel and then subjected to a CoMFA analysis. Both the parallel and perpendicular arrangements of the aromatic rings are seen in X-ray structures of SP antagonists and have been proposed as candidates for the receptor-bound conformation. The parallel (or stacked) conformation yielded a poorer correlation with a cross-validated $r^2 = 0.57$, a conventional $r^2 = 0.90$, and a predictive $r^2 = 0.78$. Our results indicate that although both alignments could generate a reasonable CoMFA correlation, the stacked conformation is unlikely to be the receptor-bound conformation, as the covalent structure of the antagonists precludes a common geometry in which the aromatic rings are stacked.

Introduction

Substance P (SP), a peptide neurotransmitter first discovered in 1931¹ and eventually characterized in 1970 as the undecapeptide Arg-Pro-Lys-Pro-Gln-Gln-Phe-Phe-Gly-Leu-Met-NH₂,² is a member of the tachykinin family of peptides. These peptides bind to a series of three neurokinin receptors, NK₁, NK₂, and NK₃, which have selective affinity for SP, neurokinin A, and neurokinin B, respectively.³ A link between the transmission of pain, the induction of inflammatory responses as a result of noxious stimuli, and the release of SP has been established.^{4–6} These observations suggest that SP receptor antagonists may be of significant therapeutic use in the treatment of a wide range of clinical conditions, ranging from arthritis,⁷ migraine,⁸ and asthma⁹ to postoperative pain and nausea.^{10–12}

The discovery of the first selective nonpeptide SP receptor antagonist CP96345^{13,14} has catalyzed research in this area, and reports of several antagonists which belong to other structural classes have rapidly followed, e.g., CP99994,¹⁵ RP73467,¹⁶ CGP47899,¹⁷ and FK888.^{18–21} Many of these compounds share structural elements, such as two or more aromatic rings, a heteroatom which links one of these rings to the central core of the molecule, and aliphatic substituents on one of the aromatic rings.²² A number of proposals for structural

elements of the ligands essential for receptor interaction^{13,23,24} and key complementary residues at the receptor binding site²⁵ have evolved to rationalize their activity. Recent advances in molecular biology and biophysical methods which have fueled the field of structure-based design have yet to yield structures for seven-transmembrane proteins such as the NK₁ receptor. Consequently, these proposals have been driven largely from indirect methods, such as structure–activity relationship (SAR) studies based on the synthesis of analogues and mutagenesis of the SP receptor.

In the absence of detailed atomic information, one can attempt to deduce an operational model of the receptor/ligand complex that gives a consistent explanation of the known data and, ideally, provides predictive value when considering new compounds for synthesis and biological testing. Constrained Search²⁶ is a form of systematic search²⁷ in which the common three-dimensional geometry required of a set of ligands for binding to a receptor can be determined. This geometry provides an orientation rule for ligands that enables the use of three-dimensional quantitative structure–activity relationship (3D-QSAR) methods. Constrained Search has been used to define a common bound geometry for a series of angiotensin-converting enzyme inhibitors²⁶ which has subsequently been used in a comparative molecular field analysis (CoMFA)²⁸ to rationalize their inhibitory potencies.²⁹ Similarly, a predictive model has been developed for nonpeptide angiotensin-II receptor antagonists³⁰ based upon a pharmacophore geometry identified by systematic search.

* To whom correspondence should be addressed.

[†] Center for Molecular Design.

[‡] Department of Computer Science.

[§] Present address: MetaPhore Pharmaceuticals, Inc., 3655 Vista Ave, St. Louis, MO 63110.

In this paper, we use Constrained Search to derive a hypothesis for the receptor-bound conformation of SP antagonists bound to the NK₁ receptor. This hypothesis is then used in CoMFA to develop a 3D-QSAR model for the antagonist binding site and to predict successfully the activity of other SP antagonists.

Results and Discussion

Pharmacophore Detection and Alignment of SP Antagonists. Constrained Search was used in an exhaustive conformational analysis to determine a common three-dimensional pattern for a set of pharmacophoric elements held by 17 representative SP antagonists (Table 1, data set = CS and ST). Starting with one ligand, intramolecular distances between essential functional groups over all sterically allowed conformations were recorded and used to constrain the search of the next ligand in the set and so on, until all that remained was a set of intramolecular distances (the IMap) that can be adopted by all of the ligands when bound to the receptor.

The Constrained Search study focused on the aromatic rings present in all of the SP antagonists and the alkyl substituents on one of these rings (Figure 1). Although a heteroatom linking one of the aromatic rings to the core of the molecule has been implicated as an important element of the pharmacophore, mutagenesis studies reveal divergent effects on affinity, depending on whether the heteroatom is a N or an O.³¹ Consequently, we opted for a conservative definition of the pharmacophore that excluded the heteroatom site. SAR studies have consistently identified alkyl substituents on the aromatic ring as affinity enhancers, and we chose to add that component to our model as well.³²⁻³⁴

Our initial Constrained Search analysis revealed that the set of 17 antagonists could not simultaneously fit all 7 elements of the pharmacophore shown in Figure 1. Positions of centroid G could not be found for compounds containing an aromatic methyl/fluoromethyl side chain that were compatible with the position of centroid G in compounds containing an aromatic methoxy side chain. This forced us to develop a strategy (outlined in Figure 2) in which the antagonists were separated into two classes (aromatic methyl/fluoromethyl side chain versus aromatic methoxy side chain), and the IMap was contracted to 6 elements or expanded to 7 elements (see Methods) as needed in order to incorporate valuable geometric information involving the seventh pharmacophore element (centroid G) into our model without requiring that all of the molecules simultaneously fit all 7 pharmacophore elements.

A Constrained Search of the antagonists using a 6-element pharmacophore in which centroid G (Figure 1) was disabled led to 2087 common alignments (IMap points) of the aromatic rings (Figure 2). MOLf was found to be the most constrained of the series, based on the number of rotatable bonds and the number of conformations produced. When the geometries of aromatic rings in these points were examined (see Methods and Figure 3), none were found consistent with a "stacked" geometry, 53 were identified as "adjacent", 37 were identified as "T", and 1990 were identified as "L". Only 7 IMap points could not be classified in one of the four categories. Upon closer inspection, it was deter-

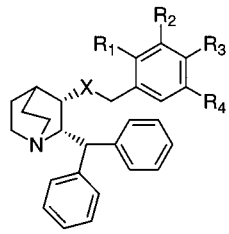
mined that the "stacked" conformations were eliminated by MOLi. No combination of isomers or conformations of MOLf and MOLi could simultaneously present a set of pharmacophore distances consistent with a "stacked" orientation of aromatic rings.

The initial 6-element pharmacophore IMap was expanded to 7 elements by increasing the resolution on distances involving the element G (the aromatic substituent centroid of Figure 1) to 0.25 Å. This increased the size of the IMap from 2087 points to 67 244. When this expanded IMap was used to constrain the six compounds in which element G was a methoxy group (MOLf, MOLa, MOLo, MOLp, CP99994, and CP96345), the resulting 7-element pharmacophore IMap retained 866 points: in 10, the aromatic rings had "T" orientations, 5 had "adjacent" orientations, and 851 had an "L" orientation. The distances spanned by the 7-element pharmacophore IMap for the aromatic methoxy compounds are summarized in Table 2.

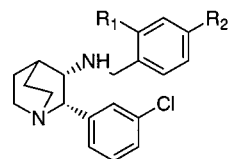
The 7-element pharmacophore IMap resulting from analysis of the methoxy subset was contracted to 6 elements and then used to constrain a search of the remaining methyl/fluoromethyl compounds. This contraction was actually done in two steps: In the first, the resolution of distances involving centroid G was increased to 8 Å, dropping the number of IMap points from 866 to 366. Next, the IMap resolution was increased to 0.25 Å, increasing the number of IMap points to 4926. These two steps effectively removed from the IMap any "memory" of constraining distances to the seventh element. When the resulting IMap was used in a Constrained Search analysis of the 11 methyl/fluoromethyl compounds, a new IMap of 410 points was produced: 6 of the IMap points were consistent with the "T" arrangement of the aromatic rings, while the remaining 404 represented a variety of "L" orientations. The actual distances spanned by these points are summarized in Table 2.

The final 7-element pharmacophore IMap was again contracted into 6 elements, resulting in 188 IMap points. When clustered in distance space, they partitioned into two distinct groups: one corresponding to a "T" conformation, the other to an "L" conformation. The same results were obtained when the order of analysis was reversed by using the original 6-element IMap first to constrain the methyl/fluoromethyl subset and then using the resulting IMap to constrain the methoxy subset. Through this series of analyses, our original 2087-point, 6-element IMap dropped to 188 points. Although the original map contained no stacked conformations, there were some adjacent conformations that could have converged to the stacked orientation upon minimization. Our analysis strategy removed these conformations from consideration and established conclusively that only conformations in which the aromatic rings have an edge-on interaction can be held in common by all of the SP antagonists.

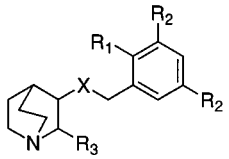
For CoMFA analysis, points in the "T" cluster were used to generate conformations. The average distance in each IMap dimension of this cluster was determined, and the IMap point closest to the average was used to generate conformations. The difference between conformations within the clusters was less than the resolution of the CoMFA grid. The first sterically valid

Table 1. Structures and Activities of SP Antagonists Used in Constrained Search and CoMFA Training Set


| molecule | X | R ₁ | R ₂ | R ₃ | R ₄ | pIC ₅₀ (M) | data set | assay | ref |
|-------------------------|------------------|---------------------------------|------------------|------------------|-----------------|-----------------------|-----------------|-----------------|-------|
| CP96345 | NH | OCH ₃ | H | H | H | 9.17 | ST ^a | IM ^d | 13,14 |
| MOLd | O | H | CF ₃ | H | CF ₃ | 8.89 | ST | CH ^e | 64 |
| Merck_BMCL_p1261_95_8a | O | H | CF ₃ | H | CF ₃ | 6.71 | CT ^b | CH | 24 |
| Merck_BMCL_p1261_95_8b | O | H | CH ₃ | H | CH ₃ | 6.53 | CT | CH | 24 |
| Merck_BMCL_p1361_93_15c | O | H | CH ₃ | H | H | 7.68 | CT | CH | 34 |
| Merck_BMCL_p1361_93_15d | O | H | H | CH ₃ | H | 6.54 | CT | CH | 34 |
| Pfizer_JMC_p2591_92_7c | NH | H | OCH ₃ | H | H | 7.70 | CT | IM | 13 |
| Pfizer_JMC_p2591_92_7d | NH | H | H | OCH ₃ | H | 6.46 | CT | IM | 13 |
| Pfizer_JMC_p2591_92_7g | NH | H | H | Cl | H | 5.72 | CT | IM | 13 |
| Pfizer_JMC_p2591_92_7h | NH | CH ₂ CH ₃ | H | H | H | 7.78 | CT | IM | 13 |
| Pfizer_JMC_p2591_92_7j | NH | NHCH ₃ | H | H | H | 7.17 | CT | IM | 13 |
| L-703605 | NH | H | H | H | H | 7.54 | CT | CH | 42,46 |
| L-705084 | NCH ₃ | OCH ₃ | H | H | H | 8.10 | CT | CH | 42,46 |
| L-703625 | O | H | H | H | H | 7.12 | CT | CH | 31 |
| L-709232 | NH | H | CF ₃ | H | CF ₃ | 8.70 | CT | CH | 31 |
| L-706125 | O | H | CH ₃ | H | CH ₃ | 9.00 | CT | CH | 31 |



| molecule | R ₁ | R ₂ | pIC ₅₀ (M) | data set | assay | ref |
|------------------------|------------------|------------------|-----------------------|----------|-------|-----|
| MOLa | OCH ₃ | OCH ₃ | 8.04 | ST | IM | 32 |
| Pfizer_BMCL_p839_94_5g | Cl | H | 6.64 | CT | IM | 32 |



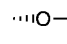
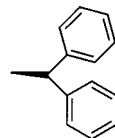
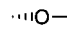
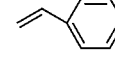
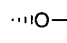
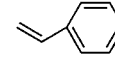
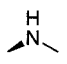
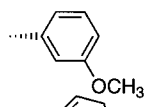
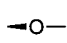
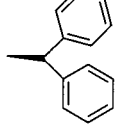
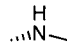
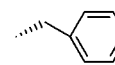
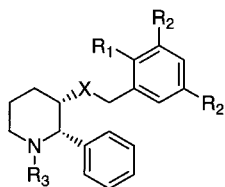
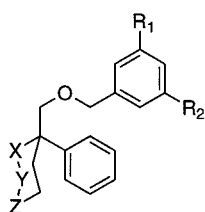
| molecule | X | R ₁ | R ₂ | R ₃ | pIC ₅₀ (M) | data set | assay | ref |
|------------------------|-------------------------------------------------------------------------------------|------------------|-----------------|--------------------------------------------------------------------------------------|-----------------------|----------|-------|-------|
| MOLe |  | H | CF ₃ |  | 9.15 | ST | CH | 64 |
| Merck_BMCL_p1261_95_6 |  | H | CH ₃ |  | 5.09 | CT | CH | 24 |
| Merck_BMCL_p1261_95_7 |  | H | CH ₃ |  | 6.89 | CT | CH | 24 |
| Merck_BMCL_p839_94_5f |  | OCH ₃ | H |  | 5.85 | CT | CH | 32 |
| Merck_BMCL_p1703_93_11 |  | H | CF ₃ |  | 6.24 | CT | CH | 64 |
| L-703766 |  | OCH ₃ | H |  | 6.63 | CT | CH | 42,46 |

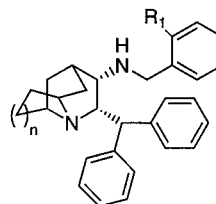
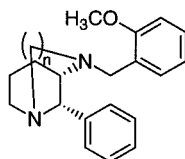
Table 1 (Continued)



| molecule | X | R ₁ | R ₂ | R ₃ | pIC ₅₀ (M) | data set | assay | ref |
|----------|----|------------------|-----------------|----------------|-----------------------|----------|-------|-------|
| CP99994 | NH | OCH ₃ | H | H | 9.77 | ST | IM | 15 |
| MOLh | O | H | CF ₃ | | 9.40 | ST | CH | 65 |
| L-733060 | O | H | CF ₃ | H | 9.00 | CT | CH | 65,66 |
| L-736281 | O | H | CF ₃ | | 8.89 | CT | CH | 65 |

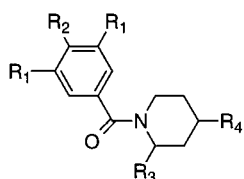


| molecule | X | Y | Z | R ₁ | R ₂ | pIC ₅₀ (M) | data set | assay | ref |
|-----------------------|-----------------|-----------------|-----------------|-----------------|-----------------|-----------------------|----------|-------|-----|
| MOLI | NH | CH ₂ | CH ₂ | CF ₃ | CF ₃ | 9.00 | ST | CH | 23 |
| MOLm | CH ₂ | NH | CH ₂ | CF ₃ | CF ₃ | 7.70 | ST | CH | 23 |
| MOLn | CH ₂ | CH ₂ | NH | CF ₃ | CF ₃ | 9.02 | ST | CH | 23 |
| Merck_JMC_p1264_95_16 | CH ₂ | CH ₂ | NH | CF ₃ | H | 7.24 | CT | CH | 23 |
| Merck_JMC_p1264_95_17 | CH ₂ | CH ₂ | NH | CH ₃ | CH ₃ | 8.05 | CT | CH | 23 |
| Merck_JMC_p1264_95_19 | CH ₂ | CH ₂ | NH | H | H | 5.96 | CT | CH | 23 |

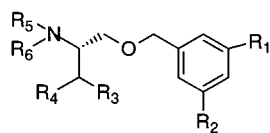


| molecule | n | pIC ₅₀ (M) | data set | assay | ref | molecule | n | R ₁ | pIC ₅₀ (M) | data set | assay | ref |
|----------|---|-----------------------|----------|-----------------|-----|-------------------------|---|------------------|-----------------------|----------|-------|-----|
| MOLo | 1 | 9.21 | ST | BH ^f | 67 | Pfizer_JMC_p2831_94_10a | 1 | H | 7.17 | CT | BH | 47 |
| MOLp | 2 | 9.44 | ST | BH | 67 | Pfizer_JMC_p2831_94_10b | 2 | H | 6.77 | CT | BH | 47 |
| | | | | | | Pfizer_JMC_p2831_94_11a | 1 | OCH ₃ | 9.04 | CT | BH | 47 |

Table 1 (Continued)

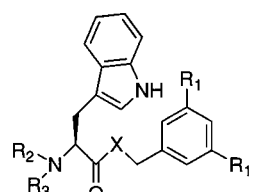


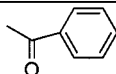
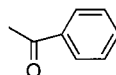
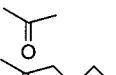
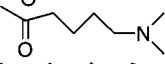

| molecule | R ₁ | R ₂ | R ₃ | R ₄ | pIC ₅₀ (M) | data set | assay | ref |
|----------|-----------------|----------------|----------------|----------------|-----------------------|-----------------|-----------------|-----|
| CGP47899 | CH ₃ | H | | | 7.82 | ST | BR ⁹ | 17 |
| CIBA_45 | Cl | H | | | 7.59 | CS ^c | BR | 68 |
| MOLi | CH ₃ | H | | | 7.52 | ST | BR | 69 |
| CIBA_1 | CH ₃ | H | | | 5.57 | CT | BR | 70 |
| CIBA_17a | CH ₃ | H | | | 6.51 | CT | BR | 70 |
| CIBA_21 | H | H | | | 5.86 | CT | BR | 68 |
| CIBA_24 | H | Cl | | | 5.86 | CT | BR | 68 |

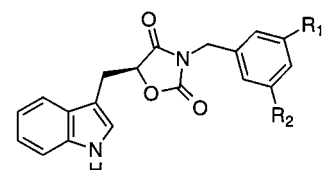
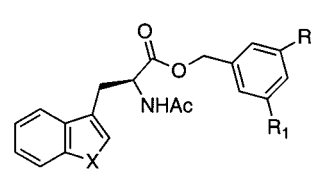


| molecule | R ₁ | R ₂ | R ₃ | R ₄ | R ₅ | R ₆ | pIC ₅₀ (M) | data set | assay | ref |
|------------------------|-----------------|-----------------|----------------|----------------|-----------------|-----------------|-----------------------|----------|-------|-------|
| MOLc | CF ₃ | CF ₃ | | | H | | 9.28 | ST | CH | 33 |
| Merck_BMCL_p1903_94_8a | H | H | | | H | H | 6.44 | CT | CH | 33 |
| Merck_BMCL_p1903_94_8b | Cl | H | | | H | H | 7.12 | CT | CH | 33 |
| Merck_BMCL_p1903_94_8e | CF ₃ | CF ₃ | | | H | H | 7.97 | CT | CH | 33 |
| Merck_BMCL_p1903_94_13 | CH ₃ | CH ₃ | | | H | | 7.09 | CT | CH | 33 |
| Merck_BMCL_p1903_94_15 | CH ₃ | CH ₃ | | | CH ₃ | CH ₃ | 8.26 | CT | CH | 33 |
| L-732106 | CF ₃ | CF ₃ | | | CH ₃ | CH ₃ | 8.70 | CT | CH | 33,71 |
| Merck_BMCL_p2161_94_1f | CH ₃ | CH ₃ | | H | H | H | 5.63 | CT | CH | 72 |
| Merck_BMCL_p2161_94_1g | CH ₃ | CH ₃ | | H | H | H | 5.63 | CT | CH | 72 |

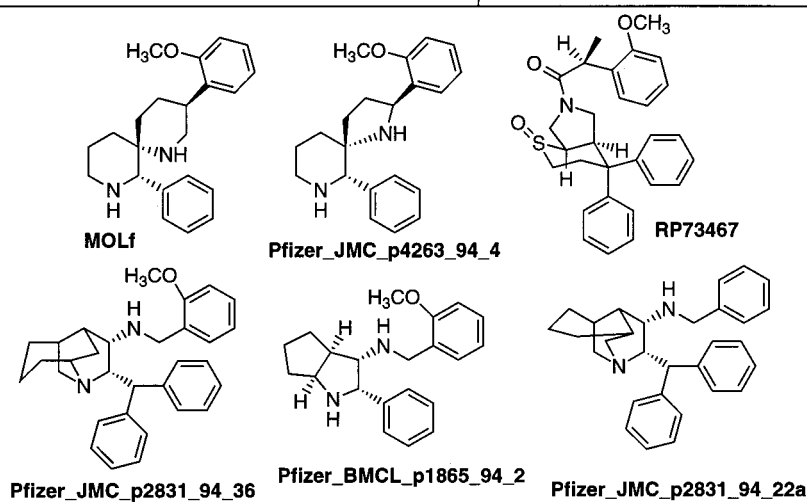
Table 1 (Continued)



| molecule | X | R ₁ | R ₂ | R ₃ | pIC ₅₀ (M) | data set | assay | ref |
|------------------------|-----------------|-----------------|-----------------|-----------------------------------------------------------------------------------|-----------------------|----------|-------|-----|
| Merck_JMC_p1269_94_15a | O | CH ₃ | H |  | 7.66 | CT | CH | 35 |
| Merck_JMC_p1269_94_10 | O | CH ₃ | CH ₃ | CH ₃ | 6.26 | CT | CH | 35 |
| Merck_JMC_p934_95_9 | NH | CH ₃ | H |  | 5.83 | CT | CH | 43 |
| Merck_JMC_p934_95_16a | CH ₂ | CF ₃ | H |  | 8.51 | CT | CH | 43 |
| Merck_JMC_p934_95_16e | CH ₂ | CF ₃ | H |  | 9.22 | CT | CH | 43 |
| Merck_JMC_p934_95_16l | CH ₂ | CF ₃ | H |  | 9.77 | CT | CH | 43 |

| molecule | R ₁ | R ₂ | pIC ₅₀ (M) | data set | assay | ref | molecule | X | R ₁ | pIC ₅₀ (M) | data set | assay | ref |
|----------------------|-----------------|-----------------|-----------------------|----------|-------|-----|----------|----|-----------------|-----------------------|----------|-------|-----|
| L-732244 | CF ₃ | CF ₃ | 7.59 | ST | CH | 37 | L-732138 | NH | CF ₃ | 8.49 | CT | CH | 37 |
| Merck_JMC_p923_95_16 | CF ₃ | H | 5.57 | CT | CH | 37 | L-708568 | NH | CH ₃ | 7.28 | CT | CH | 41 |
| Merck_JMC_p923_95_17 | H | H | 5.22 | CT | CH | 37 | L-709400 | S | CF ₃ | 7.82 | CT | CH | 41 |



| molecule | pIC ₅₀ (M) | data set | assay | ref |
|-------------------------|-----------------------|----------|-------|-----|
| MOLf | 8.70 | ST | BH | 38 |
| Pfizer_JMC_p4263_94_4 | 5.00 | CT | BH | 38 |
| Pfizer_JMC_p2831_94_22a | 6.64 | CT | BH | 47 |
| Pfizer_JMC_p2831_94_36 | 8.72 | CT | BH | 47 |
| Pfizer_BMCL_p1865_94_2 | 8.62 | CT | IM | 44 |
| RP73467 | 7.64 | CT | IM | 16 |

^a ST, used in constrained search and CoMFA training set. ^b CT, used only in CoMFA training set. ^c CS, used only in constrained search. ^d IM, binding affinity for the NK₁ receptor in human IM-9 cells using [³H]SP as ligand. ^e CH, binding affinity for the NK₁ receptor in CHO-expressed hNK₁ using [¹²⁵I]SP. ^f BH, binding affinity for the NK₁ receptor in human IM-9 cells using [¹²⁵I]Bolton-Hunter SP. ^g BR, binding affinity for the NK₁ receptor in bovine retina using [³H]SP.

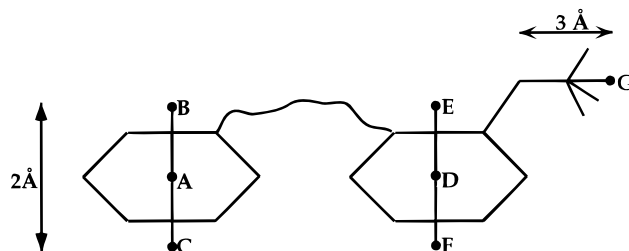


Figure 1. Pharmacophore elements used for monitoring intramolecular distances during Constrained Search analysis of SP antagonists and for alignment of molecules prior to CoMFA analyses.

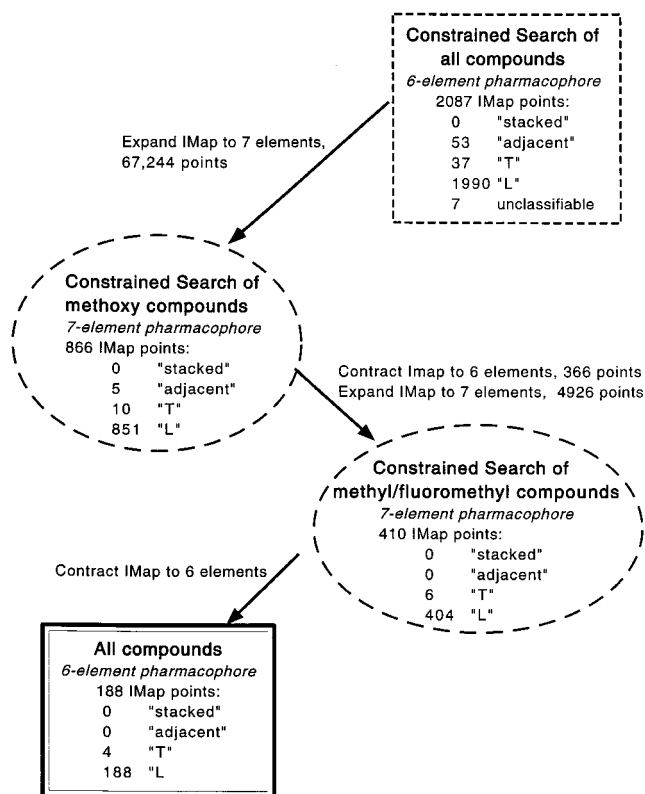


Figure 2. Schematic showing the Constrained Search strategy employed to develop an IMap that covered the entire set of 17 SP antagonists but required that only 6 of 7 pharmacophore elements be simultaneously superimposable. The results are not dependent on the order in which the analysis was done, as swapping the position of the methyl/fluoromethyl compounds and the methoxy compounds in the sequence produces the same results.

conformation identified for each molecule was used in the CoMFA analysis. The overlaid molecules are shown in Figure 4.

The "T" or edge-on orientation of the aromatic rings identified by Constrained Search in Figure 4 is quite similar to a conformation seen in the X-ray structure of an NK₁ antagonist.¹³ An alternative conformation seen in X-ray crystal structures and solution conformations of some antagonists has the aromatic rings in the parallel or stacked orientation^{13,35-37} that was eliminated in our Constrained Search analyses. This conformation has also been proposed as the bound conformation of these ligands.^{15,38} Recently, Natsugari et al. superimposed low-energy conformers of a pyrido[3,4-*b*]pyridine SP antagonist (IC₅₀ = 7.0 nM) on those of CP99994.³⁹ The conformer having the largest intersection volume with CP99994 was similar to the T conformation identified in this study by Constrained Search.

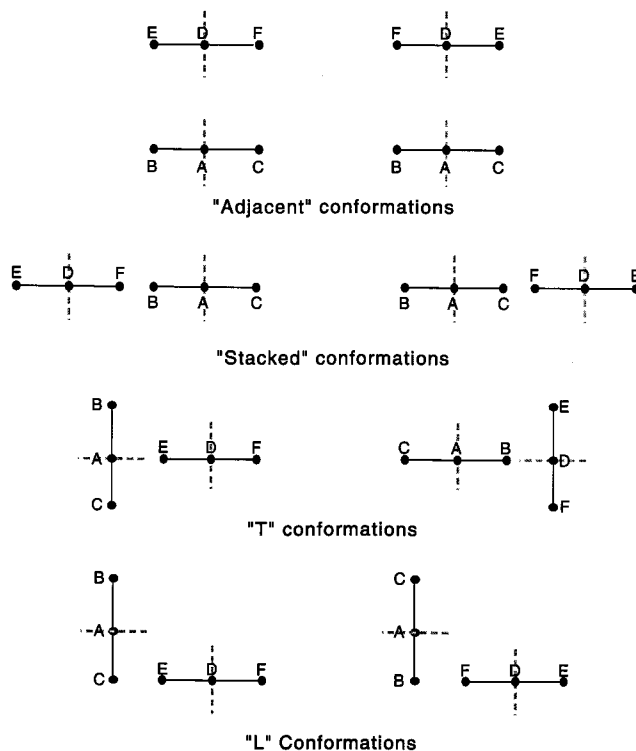


Figure 3. Diagram of aromatic ring orientations used to classify IMap points common to SP antagonists. The black lines represent normals through each of the aromatic rings, the gray dashed lines represent the plane of the aromatic rings, and the labeled points correspond to the pharmacophore elements shown in Figure 1.

The conformer having the next largest intersection volume was similar to the stacked. Notably, several molecules in our analysis (MOLo, MOLp, MOLi, and CGP47899) were unable to adopt the parallel or stacked conformation. For MOLi and CGP47899, the amide bond linking the 3,5-dimethylphenyl ring and the piperazine ring is simply too restricting.

CoMFA Analyses. We developed two CoMFA models: one based on the alignment derived from Constrained Search with the two aromatic rings in an edge-on interaction and the other based on an X-ray structure of an NK₁ antagonist³⁶ in which the rings are parallel or stacked (Methods). The results of these CoMFA analyses are summarized in Table 3. The initial analysis based on the Constrained Search alignment yielded a cross-validated $r^2 = 0.70$ and a conventional $r^2 = 0.93$ using five principal components (see also Supporting Information). The CoMFA analysis based on the stacked conformation seen in the antagonist X-ray crystal structure³⁶ yielded a poorer correlation with a cross-validated $r^2 = 0.57$ and a conventional $r^2 =$

Table 2. Summary of Commonly Held Distances between 7 Pharmacophore Elements in 17 High-Affinity SP Antagonists Determined Using Constrained Search

| distance pair ^a | internuclear distances in methoxy series | | internuclear distances in methyl/fluoromethyl series | |
|----------------------------|------------------------------------------|---------|------------------------------------------------------|---------|
| | min (Å) ^b | max (Å) | min (Å) ^b | max (Å) |
| AD | 4.75 | 6.75 | 4.75 | 6.75 |
| BD | 4.00 | 7.50 | 4.00 | 7.50 |
| CD | 4.00 | 7.75 | 4.00 | 7.50 |
| AE | 4.25 | 7.25 | 4.75 | 7.25 |
| BE | 4.00 | 8.00 | 4.00 | 7.75 |
| CE | 4.00 | 8.00 | 4.00 | 7.75 |
| AF | 4.75 | 6.75 | 4.75 | 6.75 |
| BF | 4.00 | 7.75 | 4.00 | 7.50 |
| CF | 4.00 | 7.75 | 4.00 | 7.50 |
| AG | 6.75 | 10.25 | 6.75 | 10.50 |
| BG | 6.50 | 11.00 | 6.00 | 11.25 |
| CG | 6.00 | 11.00 | 6.00 | 11.25 |

^a See Figure 1 for a definition of pharmacophore elements.^b IMap resolution = 0.25 Å.

= 0.90 using five principal components (see also Supporting Information). These values are surprisingly good, given that the training set includes many structural classes: quinuclidine, piperidine, acyclic ether, perhydroisoindol, piperazine, and tryptophan esters.

The penultimate test of a model is in its predictive power, purported to be reflected by the cross-validated r^2 . In fact, the potential strength of CoMFA is that it can be used to prioritize synthetic targets by activity, or to identify and computationally screen novel scaffolds. After developing the two CoMFA models, biological activities for a set of new compounds (Table 4) were obtained from A. Giolitti (A. Menarini) and a recent publication.⁴⁰ The former are all analogues of FK888^{18–21} and do not have the bis-trifluoromethyl, bis-methyl, or methoxy aromatic ring substitutions thought to be important in the training set. When the CoMFA model based on the "T" or edge-on conformation identified by Constrained Search was used to predict the activities of these 18 new SP antagonists, the predictive r^2 was 0.82. The CoMFA model based on the stacked aromatic ring conformation seen in an X-ray crystal structure produced a slightly poorer predictive r^2 of 0.78 for the same test set (see Supporting Information). Our results, based on an exhaustive conformational analysis and CoMFA, are consistent with previous modeling studies favoring the T conformation.³⁹ A visual examination of the two CoMFA models revealed that the one based on the X-ray structure had contours which were more diffuse than those observed in the T or edge-on model. This is most likely a consequence of the poorer alignment of antagonists in the stacked model (see Methods and Supporting Information).

Do the CoMFA models make chemical sense based on what we know about SP antagonists? The CoMFA electrostatic and steric fields from the Constrained Search alignment ("T" or edge-on) are presented as contour plots in Figure 5. The field values were calculated as the scalar product of the β -coefficient and the standard deviation associated with a particular column in the QSAR table (STDEV*COEFF). The values corresponding to electrostatic columns are plotted as the percentage of contribution to the QSAR equation. In Figure 5, the red contours represent regions of decreased tolerance for positive charge (20% contribu-

tion), while the blue contours represent regions of increased tolerance for positive charge (80% contribution).

In Figure 5, the electrostatic contours on the methoxy substituent oxygen and in its vicinity are consistent with the enhanced activity seen with this substituent. The electrostatic contours in the vicinity of the phenyl meta-substituent suggest that trifluoromethyl is preferred over methyl or hydrogen in this location. Site-directed mutagenesis studies of the NK₁ receptor suggest that the bis-trifluoromethyl-benzyl ester moieties in L-732138 interact with His 265 in the sixth putative transmembrane spanning region of the receptor.⁴¹ In the upper left part of Figure 5, the small electrostatic spot in the vicinity of the C-3 nitrogen atom of CP96345 indicates that a heteroatom, either nitrogen in CP96345 or oxygen in the ethers such as MOLd, is preferred at this site. Site-directed mutagenesis data for the NK₁ receptor reveals that Gln 165, on the fourth transmembrane domain, is involved in the binding of quinuclidines having an O or NH group at C-3 in CP96345, possibly through a hydrogen bond between these groups and Gln 165.⁴² Replacing Gln 165 for alanine in the human receptor caused a 40–44-fold reduction in affinity for these compounds. In contrast, the binding of *N*-acetyl-tryptophan esters to the Gln 165 Ala mutant was measured and found to be little changed from affinities for the wild-type receptor, indicating that this class of antagonists does not rely on the side chain of residue 165 for binding.⁴³ Similarly, the ketone analogue (Merck_JMC_p934_95_16a, Table 1) of one of the tryptophan esters had affinity at the mutant receptor which was only 5-fold lower than at the wild-type receptor. When higher-affinity ketone analogues of tryptophan esters were tested at the mutant receptor, all exhibited a reduction in affinity, but this varied from only 2-fold to 25-fold.⁴³ These data suggest that the ketone carbonyl in the *N*-acetyl-tryptophan ester series does not bind to the same residue as the exocyclic heteroatom in the quinuclidine antagonists and that Gln 165 may contribute either directly or indirectly to the higher-affinity binding of some of these ligands but is not essential to the activity of the *N*-acetyl-tryptophan ester series as a whole.⁴³ This suggestion is consistent with the fact that electrostatic contours in the vicinity of the C-3 nitrogen atom of CP96345 are small in Figure 5. The electrostatic contours in the vicinity of the quinuclidine nitrogen in CP96345 indicate that the nitrogen atom at this position is preferred. MOLm shows a 20-fold loss in affinity compared to MOLn, consistent with proposed models of antagonist binding to the NK₁ receptor in which the position of the basic nitrogen is an important feature.^{23,44,45} In Figure 5, the electrostatic contours, which indicate areas where high electron density within the ligands enhances affinity, overlap with the π -aromatic electron density of the most active compounds. These contours in the vicinity of one of the phenyl rings of the benzhydryl support the idea that only one of the phenyl rings of the benzhydryl is involved in receptor binding.²⁴ Substitution of His 197 in the fifth transmembrane helix of the human NK₁ receptor by different amino acids and analysis of structural analogues of antagonists suggest that His 197

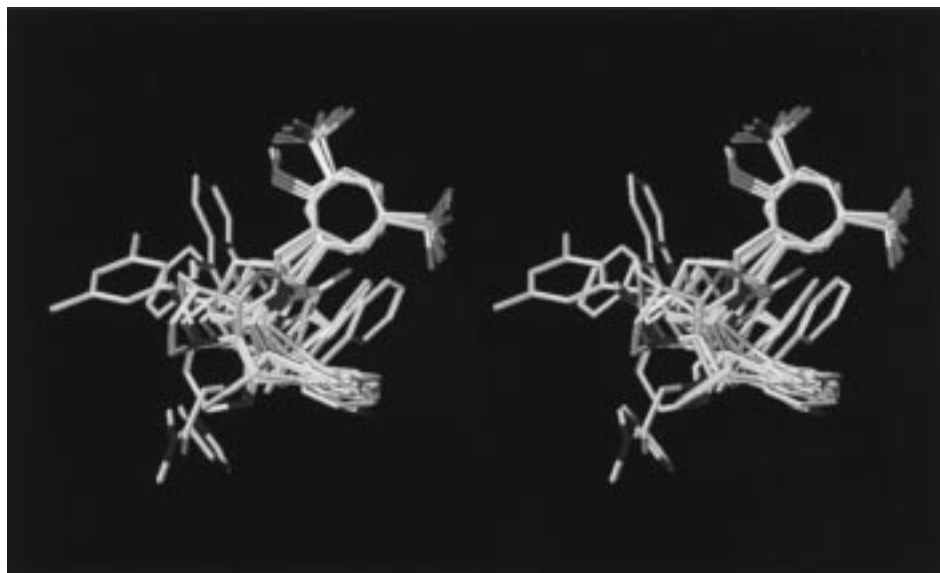


Figure 4. Overlaid conformations of each of the 17 SP antagonists that fit the final IMap of Figure 2.

Table 3. Summary of Results from CoMFA of 73 SP Antagonists Using Two Different Alignments: One Derived from a Constrained Search Analysis in Which the Aromatic Rings Are in a "T" or Edge-On Interaction and the Other Based on an X-ray Structure of an SP Antagonist in Which the Rings Are "Stacked" or in a Face-to-Face Interaction

| QSAR alignment | $r^2_{\text{cross}}^a$ | r^2^b | no. of components | F | SE |
|-----------------------------------------------------------|------------------------|---------|-------------------|-----|------|
| Constrained Search ("T" or edge-on ^c) | 0.70 | 0.93 | 5 | 174 | 0.36 |
| X-ray structure ("stacked" or face-to-face ^c) | 0.57 | 0.90 | 5 | 123 | 0.42 |

^a Cross-validated r^2 : r^2 value for analysis using designated number of cross-validation groups. ^b Conventional r^2 : fitted r^2 value for predictive model derived using no cross-validation and the optimum number of principal components. ^c Defined in Figure 3.

is involved in an amino–aromatic interaction with the benzhydryl moiety of CP96345.⁴⁶

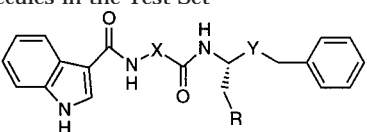
The steric contribution contour plot from the analysis based on the Constrained Search alignment is plotted as the STDEV*COEFF field in Figure 6. In Figure 6, the green contours represent regions of high steric tolerance (80% contribution), while the yellow contours represent regions of low steric bulk tolerance (20% contribution). Areas of high steric bulk tolerance are noted in the vicinity of the *o*-methoxy substituent or at the meta-position of the phenyl. These substituent positions are important for affinity, with methoxy preferred as the single ortho-substituent or bis-methyl/bis-trifluoromethyl preferred for ortho,meta-disubstitution.³⁴ In Figure 6, areas of low steric bulk tolerance predict a steric wall in which added bulk will decrease potency. The observation that larger fused bridges in the quinuclidine core (Pfizer_JMC_p2831_94_10a, 10b, 11a, 22a, 36 of Table 1) caused a greater loss of receptor affinity supports the idea that the receptor forms a particularly tight binding interaction with this portion of the quinuclidine structure.⁴⁷ Figure 6 confirms these results and depicts the unfavorable receptor interactions for additional substitution projecting from the nucleus away from the bridge bearing the diphenylmethyl and benzylamine groups. Those studies suggested that these antagonists bind to similar binding sites on the NK₁ receptor and that, as proposed for

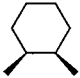
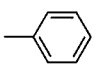
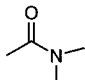
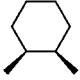
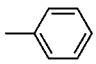
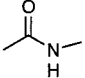
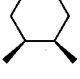
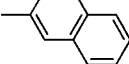
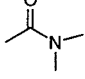
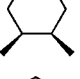
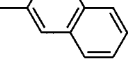
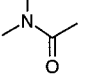

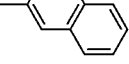
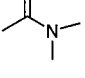
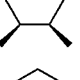
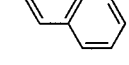
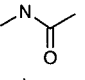
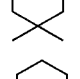
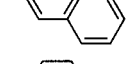
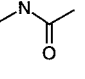
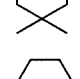
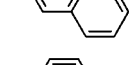
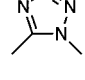
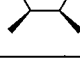
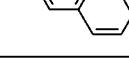
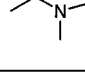
CP99994,¹⁵ its spirocyclic analogue,³⁸ and the compound by Natsugari et al.,³⁹ the relative spatial orientation of the two phenyl groups may be an important factor for binding.

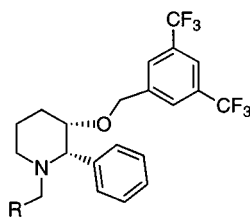
Conclusions

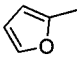
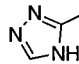
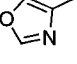
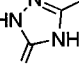
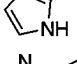
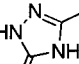
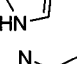
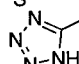
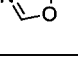
We have used Constrained Search, a systematic approach, to predict the receptor-bound conformation of the most significant portions of SP antagonists at the NK₁ receptor, by identifying a three-dimensional arrangement of pharmacophore elements which is mutually consistent for all active analogues. This arrangement, when used as an alignment rule to determine correspondence between assorted classes of antagonists, has been shown to yield a good predictive model of activity as described by CoMFA.

Over the past 5 years, receptor mutagenesis has been combined with modification of the ligand to identify specific molecular interactions between ligands and the G-protein-coupled receptors in an approach that may be thought of as two-dimensional mutagenesis.⁴⁸ By examining the additive effects of modifying functional groups on the ligand and substitution of amino acid side chains on the receptor, this two-dimensional approach allows the identification of specific interactions between the receptor and the ligand. At its limit, this combination can provide a low-resolution sketch of the interactions that dock the ligand in the receptor binding pocket. However, mutational data are not always straightforward to interpret: it has been suggested that some mutations alter the local or global conformation^{49,50} of the receptor.^{51,52} This should be kept in mind when interpreting experimental results as well as building 3D receptor models. Our results, which couple Constrained Search and CoMFA, are consistent with the two-dimensional mutagenesis results. In the absence of high-resolution structural data for G-protein-coupled receptors by X-ray crystallography or NMR, models derived from the coupling of Constrained Search and CoMFA provide information about ligand–receptor interactions that can be useful in the drug discovery process. In addition, these CoMFA results facilitate efforts to construct a 3D model of the NK₁ receptor

Table 4. Structures and Activities of the Molecules in the Test Set


| molecule ^a | X | R | Y | pIC ₅₀ (M) ^b |
|-----------------------|-------------------------------------------------------------------------------------|-------------------------------------------------------------------------------------|--------------------------------------------------------------------------------------|------------------------------------|
| MEN 10711 |  |  |  | 6.9 |
| MEN 10720 |  |  |  | 5.7 |
| MEN 10725 |  |  |  | 7.9 |
| MEN 10914 |  |  |  | 8.3 |
| MEN 10930 |  |  |  | 8.9 |
| MEN 10937 |  |  |  | 6.5 |
| MEN 11091 |  |  |  | 7.7 |
| MEN 11260 |  |  |  | 5.8 |
| MEN 11354 |  |  |  | 5.9 |



| molecule ^c | R | pIC ₅₀ (M) ^d | molecule ^c | R | pIC ₅₀ (M) ^d |
|-----------------------|-------------------------------------------------------------------------------------|------------------------------------|-----------------------|---------------------------------------------------------------------------------------|------------------------------------|
| Merck_JMC_p2907_96_3 |  | 7.4 | Merck_JMC_p2907_96_11 |  | 9.7 |
| Merck_JMC_p2907_96_4 |  | 9.0 | L-741671 |  | 10 |
| Merck_JMC_p2907_96_7 |  | 9.3 | Merck_JMC_p2907_96_14 |  | 9.1 |
| Merck_JMC_p2907_96_8 |  | 9.0 | Merck_JMC_p2907_96_17 |  | 7.4 |
| Merck_JMC_p2907_96_15 |  | 9.0 | | | |

^a Structures and activities provided by A. Giolitti of A. Menarini. ^b Binding affinity for the NK₁ receptor in human IM-9 cells using [³H]SP as ligand. ^c Taken from ref 40. ^d Binding affinity for the NK₁ receptor in CHO-expressed hNK₁ using [¹²⁵I]SP.

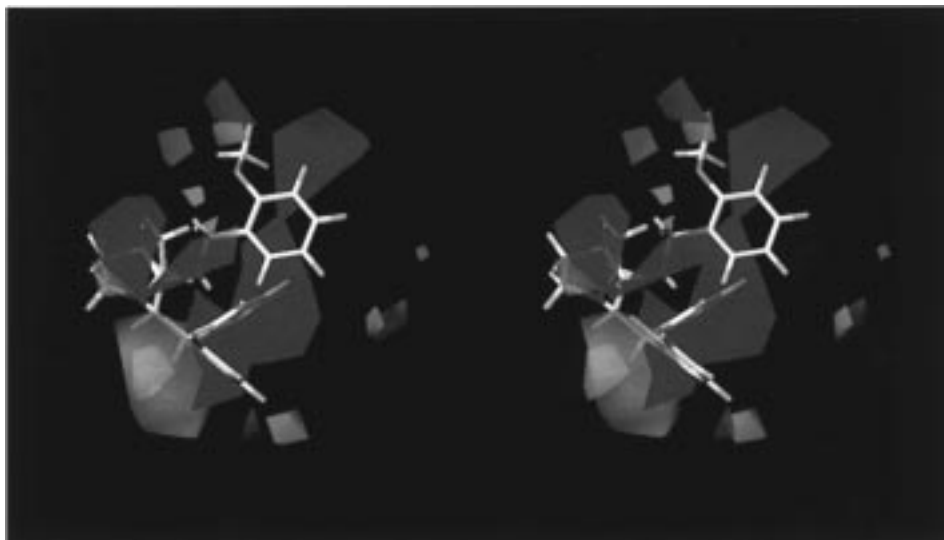


Figure 5. Crossed stereoview of CoMFA electrostatic contours from the model based on a Constrained Search alignment. Compound CP96345 is shown. The red contours (contribution level of 20%) indicate regions where the addition of negative charge will increase activity. The blue contours (contribution level of 80%) indicate regions where the addition of positive charge will increase activity.

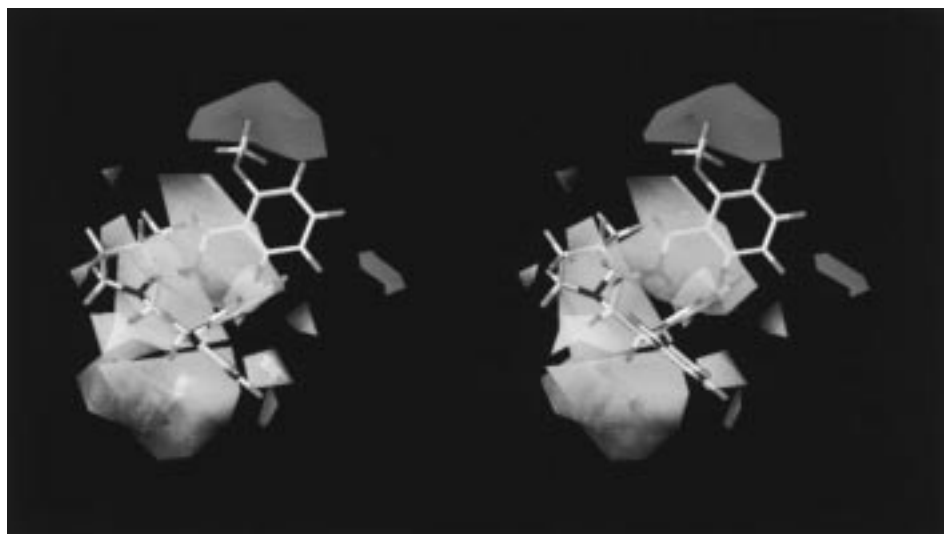


Figure 6. Crossed stereoview of CoMFA steric contours from the model based on a Constrained Search alignment. Compound CP96345 is shown. The green contours (contribution level of 80%) indicate regions where the addition of steric bulk is allowed and also define the steric boundary of the active site. The yellow contours (contribution level of 20%) indicate regions where the addition of steric bulk is associated with decreased activity.

which will further refine our understanding of receptor–ligand interaction.

Methods

A. Constrained Search. 1. Molecules and Their Geometries. The 17 SP antagonists employed in Constrained Searches are shown in Table 1 (data set = ST and CS). Each was chosen primarily for its combination of interesting conformational properties and high affinity for the NK₁ receptor. In cases where biological data was available only for racemic mixtures, both enantiomers were considered in separate analyses.

Molecules were built using the fragment library and sketch module within SYBYL.⁵³ Because systematic search uses a rigid geometry approximation,²⁷ a good starting geometry is necessary for high-quality results. Structures were minimized (300 steps) and subjected to molecular dynamics (50.9 ps) using the Tripos force field (no electrostatics). Conformations were saved every 500 fs and minimized to a gradient convergence of 0.05 kcal/(Å·mol). The lowest-energy conformation of each molecule was then minimized using the block diagonal New-

ton–Raphson method in MM3⁵⁴ to the default energy convergence of 0.000 08 kcal/(Å·mol) per atom.

2. Pharmacophore Definition. Centroids were defined for all aromatic rings (A and D of Figure 1), and for each aromatic ring, a normal to the plane of the ring was constructed through the centroid. The dummy atoms defining the normal (B, C, E, and F of Figure 1) were 1 Å away from the centroid of the ring. The centroid for pharmacophore methyl/fluoromethyl groups (G of Figure 1) was calculated using the hydrogens or fluorines of the group. This was then linked to the heavy atom penultimate to the group by a 3-Å dummy bond—e.g., for methoxy groups, the centroid of the methyl hydrogens was determined, bonded to the oxygen, and the O–Du bond was extended to a distance of 3 Å along the O–C axis.

When molecules contained more than two aromatic rings (for example, CP96345), centroids and normals were constructed for all of the aromatic rings. In some cases the correspondence between one pair of aromatic rings on different molecules was clear from the connectivity but was not obvious for the second pair (as in the benzhydryl portion of CP96345).

In these cases, all possible pairings of the aromatic rings were considered to determine which was likely to define the pharmacophore. In every case, these pairings did not reduce the number of IMap points, meaning that no single mapping was preferred. Because there was no preferred mapping, we arbitrarily selected the *proS* aromatic ring for the pharmacophore. For the aromatic ring bearing the fluoromethyl/methoxy substituent, the normals were labeled such that looking down the sp^3 - sp^2 bond from the core of the molecule into the aromatic ring, the nearest methoxy substituent was on the left and the top normal corresponded to element E. This is consistent with the view shown in Figure 1.

3. Systematic Search Parameters. Conformational analyses were performed using the Constrained Search option in Receptor 3.2⁵⁵ and four of the eight processors on an SGI 4d/380S. Torsion ranges on all angles were 0–359° with the exception of amides ($\pm 10^\circ$ from cis and trans conformations) and symmetric rotors (0–120° for methyl and fluoromethyl groups). The results of the analyses were similar for IMap resolutions of either 0.125 or 0.250 Å, and consequently only the results at 0.250 Å are reported. Two different sets of general van der Waals scaling factors were used: 0.92, 0.84, and 0.65 (for general, 1–4, and H-bonding interactions, respectively) with a hydrogen radius of 0.75 Å and 0.90, 0.82, and 0.65 with a hydrogen radius of 0.5 Å. The results were the same for the two sets of parameters.

Adaptive sampling,²⁷ an option in which search grid points are repositioned to ensure that all allowed ranges are adequately sampled, was employed. Radial sampling, using a search grid in distance space²⁷ rather than torsion space, was also used to address the over- or undersampling of Cartesian space which occurs when the same torsion angle increment is used for groups having different rotating arm lengths. Torsional and steric energies for each aggregate on either side of every rotatable bond were determined at 2° increments and the mean values computed. For each rotatable bond, angle ranges in which the torsional or steric energy was more than 20% higher than the bond's mean were not further considered in the search.

Radial increments of 0.125 or 0.250 Å were employed for all nonring torsions. With the exception of the quinuclidine cage structure, all ring torsion angles were allowed to rotate (closure tolerances: ± 0.05 Å for ring closure bond and 1,3 distances spanning the closure bond and $\pm 5^\circ$ for bond angles on either side of the closure bond). Molecules containing flexible ring(s) were preprocessed by extracting the ring(s) and solving for torsions that would produce closed, cyclic structures at an increment of 0.0625 Å or less (equivalent on average to a 2.3° angle increment). The resulting torsions (as tuple files) were used to constrain the corresponding molecule in the Constrained Search analysis.

In initial trial analyses, molecules were subjected to a coarse unconstrained systematic search (radial scan factor = 1.5 Å) in order to determine their relative torsional freedom. Molecules were ordered based on their degree of conformational freedom, and Constrained Searches were done on molecules in that sequence, with the most constrained molecules being searched first. All runs prior to the final production run used only the "core" rotations, e.g., the torsions linking the pharmacophoric groups.

4. IMap Expansion and Contraction. In cases where all molecules of a given set fail to adopt a common geometry for all of the pharmacophore elements, the IMap will contain zero points. In these cases, elements of the pharmacophore can be deleted, or alternatively, the IMap can be contracted by decreasing the resolution for distances involving one or more elements (for example, to 8 Å). By retaining the definition of the element in the IMap, but decreasing its resolution, the element can be still be invoked in later stages of the analysis simply by increasing the resolution of distances involving that element. For an existing IMap, contraction results in a decrease in the number of points, while expansion results in an increased number of points. The ability to contract and expand IMaps allows the construction of 3D

pharmacophore maps without requiring that all of the molecules simultaneously fit all of the pharmacophore elements.

5. Analysis of IMap Points. A C program was written which analyzed IMap points to determine the relative orientation of the aromatic rings in their associated conformations ("T", "L", "stacked", or "adjacent" as defined in Figure 3). These classifications used all of the pairwise distances between the rings (AE, AD, AF, BD, BE, BF, CD, CE, and CF of Figure 1) and simple geometric criteria: for example, in the case of the "T"-type conformations, BE = CE, BD = CD, BF = CF, and AF > AD > AE. Tolerances in these determinations were the same as the resolution of the IMap, 0.25 Å. The "T" and "L" orientations were edge-on interactions, while the "stacked" orientation had both rings parallel as shown in Figure 3. The "adjacent" structures were those in which the planes of the rings were parallel but not stacked on top of each other. Binning of IMap points was done sequentially, with "stacked" structures identified first, "adjacents" identified from the remaining structures, and "T" and "L" structures identified in subsequent steps.

B. CoMFA. 1. The Two CoMFA Models. All molecular modeling and CoMFA²⁸ studies were performed on a Silicon Graphics Iris Indigo R4000 computer running SYBYL 6.1a.⁵³ A training set of 72 molecules (Table 1) was selected from the literature, spanning the diversity of antagonist structures and activities. In the first study, the alignment identified by Constrained Search was used to superpose molecules. Structures in the training set were matched to the template from the Constrained Search which most closely resembled their structure. For molecules whose biological activity was reported for a mix of stereoisomers (L-703625, L-709232, and L-706125), the isomer that best fit the template was used, and its stereochemistry is shown in Table 1. The template molecules were defined to be fixed aggregates, and within SYBYL MULTIFIT, constraints were defined which forced superimposition of the training set molecule's pharmacophore groups onto the template's corresponding groups. The constraints had force constants of 20 kcal/mol-Å² and involved carbons of the aromatic rings and methyl/fluoromethyl/methoxy groups (if present). The TRIPOS force field⁵⁶ was used with no electrostatics, and the fit was done for 100 steps. Following the fitting, the pharmacophore groups of each training set molecule (two aromatic rings plus methyl/fluoromethyl/methoxy) were defined as a fixed aggregate and each structure was minimized. Only the pharmacophoric groups were used to constrain the orientation of molecules, and portions of molecules which were not uniquely determined by the pharmacophoric constraints were allowed to find their own local minima without any attempt to optimize any other feature such as volume overlap.

All molecules were assigned a formal charge of 0, and point charges for atoms in the training set were calculated using MOPAC 6.0⁵⁷ and the AM1 model Hamiltonian⁵⁸ (keywords: 1SCF, MMOK). The molecules were then input as rows of a QSAR table along with their respective affinities (shown in Table 1). With the exception of MOLf, Pfizer_JMC_p4263_94_4, and Pfizer_BMCL_p1865_94_2, binding affinity is expressed as pIC_{50} . In these cases, the affinity was reported as K_i , and the values of S and K_m (see Appendix), needed for converting K_i to IC_{50} , were not available in the primary references. If we assume $K_m = 0.5$ nM and $S = 0.07$ nM, $IC_{50} = K_i \times 1.14$. Although biological data for the antagonists used in the CoMFA analyses comes from different sources, in general there is good agreement in affinities across laboratories when the same ligand is evaluated. Specifically, IC_{50} values for CP96345 have been reported as 0.77 nM in IM-9 cells,¹³ 0.5 nM in COS cells,⁴² and 0.4 nM in CHO cells.³⁵ Similarly, K_i values for CP99994 have been reported as 1.5 nM in IM-9 cells⁴⁴ and 0.4 nM in COS cells.⁵⁹

CoMFA steric and electrostatic fields were calculated using a distance-dependent dielectric and entered as columns in the QSAR table. Regression analyses were done using the SYBYL implementation of the PLS algorithm,⁶⁰ initially with cross-validation (the leave-one-out technique) and five principal

components. The optimal number of components to be used in conventional analyses was chosen from the analysis with the highest cross-validated r^2 value, and for component models with identical r^2 values, the model with the smallest standard error of prediction. To improve the signal-to-noise ratio, the leave-one-out calculations were performed with a 2.0 kcal/mol energy column filter.

In the second alignment evaluated by CoMFA, the strategy outlined above was used to align training set structures to the conformation of a CP96345 analogue observed by X-ray.³⁶ Coordinates for this template (refcode=LEWCUL) were obtained from the Cambridge Structural Database.⁶¹ In this template, the two key aromatic rings adopt a stacked or parallel interaction with each other. SYBYL MULTIFIT was used to align structures, with the constraints involving elements used in the Constrained Search. In this model, the alignment of structures was not as tight as for the Constrained Search edge-on alignment of antagonists, simply because the covalent structure of some antagonists prohibited a perfectly stacked structure.

2. The Test Set. The predictive ability of the two CoMFA models was tested against a set of nine compounds supplied by A. Giolitti (A. Menarini) as well as a set of nine antagonists from a recent publication.⁴⁰ Structures in the test set (Table 4) were matched to a template from each CoMFA alignment which most closely resembled their structure. Using SYBYL MULTIFIT, the phenyl ring and the naphthalene ring (for example, in MEN10930) were superimposed on the methoxy phenyl ring and the *proS* phenyl ring of the diphenyl (for example, in CP96345), respectively.²² The constraints involved carbons of the aromatic rings. Following the fitting, each structure was minimized using the TRIPOS force field as described earlier.

The predictive r^2 was used to evaluate the predictive power of the two CoMFA models and was based only on molecules from the test set. Predictive r^2 is calculated using the formula:

$$\text{predictive } r^2 = 1 - (\text{"press"}/\text{SD})$$

where SD is the sum of the squared deviations between the actual activities of the compounds in the test set and the mean activity of the training set compounds and "press" is the sum of the squared deviations between predicted and actual activities for every compound in the test set. It should be obvious from the equation that prediction of the mean value of the training set for each member of the test set would yield a predictive $r^2 = 0$. This is analogous to the cross-validated r^2 definition⁶² and can result in a negative value reflecting a complete lack of predictive ability of the model for the molecules included in the test set.

Acknowledgment. The authors acknowledge support from the National Institutes of Health (GM24483). We wish to thank Dr. Alessandro Giolitti of A. Menarini (Florence, Italy) for supplying the structures and the activity data of the compounds in the test set and also Prof. James E. Krause of Department of Anatomy and Neurobiology, Washington University, for supplying the information on the value of K_m and S . We thank our colleagues such as Richard Dammkoehler whose efforts through the years have been essential to the progress described in this report as well as Stanislav Galaktionov, Richard Head, David Lewis, Gregory Nikiforovich, and Rino Ragno for helpful discussions and logistical support.

Appendix

Biological activities used in the CoMFA analyses of training and test sets are expressed as

$$\text{pIC}_{50} = -\log \text{IC}_{50} \quad (1)$$

where pIC_{50} is the transformed activity and IC_{50} is the

concentration of unlabeled ligand that causes 50% inhibition of specifically bound ¹²⁵I-labeled SP.

Biological activities for the compounds in the test set shown in Table 4 were obtained from A. Giolitti (A. Menarini) as K_i values. To obtain pIC_{50} values, the Cheng and Prusoff equation⁶³ determined for the case involving one substrate and one competitive inhibitor present was used

$$\text{IC}_{50} = K_i(1 + S/K_m) \quad (2)$$

where K_i is the dissociation constant, S is the substrate concentration, and K_m is the Michaelis constant of the substrate. This equation is valid when the velocity in the presence of the inhibitor is one-half the velocity in the absence of the inhibitor.

Based on eq 2, IC_{50} values for all compounds in the test set were determined using the K_m value of 0.5 nM, $S = 0.07$ nM (J. E. Krause, personal communication), and the corresponding K_i values (A. Giolitti, personal communication).

Supporting Information Available: Plots of predicted vs actual pIC_{50} for CoMFA analyses based on two different SP antagonist alignments; a figure of 17 overlaid SP antagonists fit to a stacked alignment of aromatic rings; and CoMFA contours (9 pages). Ordering information is given on any current masthead page.

References

- von Euler, U. S.; Gaddum, J. H. An Unidentified Depressor Substance in Certain Tissue Extracts. *J. Physiol.* **1931**, *72*, 74–87.
- Chang, M. M.; Leeman, S. E.; Niall, H. D. Amino Acid Sequence of Substance P. *Nature New Biol.* **1971**, *232*, 86–87.
- Guard, S.; Watson, S. P. Tachykinin Receptor Types: Classification and Membrane Signaling Mechanisms. *Neurochem. Int.* **1991**, *18*, 149–165.
- Maggi, C.; Patacchini, R.; Rovero, P.; Giachetti, A. Tachykinin Receptors and Tachykinin Receptor Antagonists. *J. Auton. Pharmacol.* **1993**, *13*, 23–93.
- Otsuka, M.; Yanagisawa, M. Effect of a Tachykinin Antagonist on a Nociceptive Reflex in the Isolated Spinal Cord Tail Preparation of the New-born Rat. *J. Physiol. (London)* **1988**, *395*, 255–270.
- Snider, R. M.; Lowe, J. A., III. Substance P and the Tachykinin Family of Peptides. *Chem. Ind.* **1991**, *11*, 792–794.
- Lotz, M.; Carson, D. A.; Vaughan, J. H. Substance P Activation of Rheumatoid Synoviocytes: Neural Pathway in Pathogenesis of Arthritis. *Science* **1987**, *235*, 893–895.
- Moskowitz, M. A. Neurogenic Versus Vascular Mechanisms of Sumatriptan and Ergot Alkaloids in Migraine. *Trends Pharmacol. Sci.* **1992**, *13*, 307–311.
- Barnes, P.; Belvisi, M.; Rogers, D. Modulation of Neurogenic Inflammation: Novel Approaches to Inflammatory Disease. *Trends Pharmacol. Sci.* **1993**, *11*, 185–189.
- Bouutra, C.; Bunce, K.; Dale, T.; Gardner, C.; Jordan, C.; Twissell, D.; Ward, P. Anti-emetic Profile of a Non-peptide Neurokinin NK₁ Receptor Antagonist, CP-99, 994, in Ferrets. *Eur. J. Pharmacol.* **1993**, *249*, R3–R4.
- Tattersall, F. D.; Rycroft, W.; Hargreaves, R.; Hill, R. The Tachykinin NK₁ Receptor Antagonist CP-99,994 Attenuates Cisplatin Induced Emesis in the Ferret. *Eur. J. Pharmacol.* **1993**, *250*, R5–R6.
- Tattersall, F. D.; Rycroft, W.; Hargreaves, R.; Hill, R. Enantioselective Inhibition of Apomorphine-Induced Emesis in the Ferret by the Neurokinin-1 Receptor Antagonist CP-99,994. *Neuropharmacology* **1994**, *33*, 259–260.
- Lowe, J. A., III; Drozda, S. E.; Snider, R. M.; Longo, K. P.; Zorn, S. H.; Morrone, J.; Jackson, E. R.; McLean, S.; Bryce, D. K.; Bordner, J.; Nagahisa, A.; Kanai, Y.; Suga, O.; Tsuchiya, M. The Discovery of (2S,3S)-*cis*-2-(Diphenylmethyl)-N-[(2-methoxyphenyl)methyl]-1-azabicyclo[2.2.2]octan-3-amine as a Novel, Non-peptide Substance P Antagonist. *J. Med. Chem.* **1992**, *35*, 2591–2600.
- Snider, R. M.; Constantine, J. W.; Lowe, J. A., III; Longo, K. P.; Lebel, W. S.; Woody, H. A.; Drozda, S. E.; Desai, M. C.; Vinick, F. J.; Spencer, R. W.; Hess, H.-J. A Potent Nonpeptide Antagonist of the Substance P (NK₁) Receptor. *Science* **1991**, *251*, 435–437.
- Desai, M. C.; Lefkowitz, S. L.; Thadeio, P. F.; Longo, K. P.; Snider, R. M. Discovery of a Potent Substance P Antagonist: Recognition of the Key Molecular Determinant. *J. Med. Chem.* **1992**, *35*, 4911–4913.

- (16) Achard, D.; Truchon, A.; Peyronel, J.-F. Perhydrothiopyranopyrroles Derivatives: A Novel Series of Potent and Selective Nonpeptide NK₁ Antagonists. *Bioorg. Med. Chem. Lett.* **1994**, *4*, 669–672.
- (17) Schilling, W.; Bittiger, H.; Brugger, F.; Criscione, L.; Hauser, K.; Ofner, S.; Olpe, H. R.; Vassout, A.; Veenstra, S. In *Perspectives in Medicinal Chemistry*; Testa, B., Kyburz, E., Fuhrer, W., Giger, R., Eds.; Verlag Helvetica Chimica Acta: Basel, Switzerland, 1993; pp 207–220.
- (18) Hagiwara, D.; Miyake, H.; Morimoto, H.; Murai, M.; Fujii, T.; Matsuo, M. Studies on Neurokinin Antagonists. 1. The Design of Novel Tripeptides Possessing the Glutamyl-D-tryptophylphenylalanine Sequence as Substance P Antagonists. *J. Med. Chem.* **1992**, *35*, 2015–2025.
- (19) Hagiwara, D.; Miyake, H.; Morimoto, H.; Murai, M.; Fujii, T.; Matsuo, M. Studies on Neurokinin Antagonists. 2. Design and Structure–Activity Relationships of Novel Tripeptide Substance P Antagonists, N⁶-[N⁶-(N⁶-Acetyl-L-threonyl)-N⁶-formyl-D-tryptophyl]-N-methyl-N-(phenylmethyl)-L-phenylalaninamide and its Related Compounds. *J. Med. Chem.* **1992**, *35*, 3184–3191.
- (20) Hagiwara, D.; Miyake, H.; Murano, K.; Morimoto, H.; Murai, M.; Fujii, T.; Nakanishi, I.; Matsuo, M. Studies on Neurokinin Antagonists. 3. Design and Structure–Activity Relationships of New Branched Tripeptides N⁶-(Substituted L-aspartyl, L-ornithyl, or L-lysyl)-N-methyl-N-(phenylmethyl)-L-phenylalaninamides as Substance P Antagonists. *J. Med. Chem.* **1993**, *36*, 2266–2278.
- (21) Hagiwara, D.; Miyake, H.; Higari, N.; Karino, M.; Maeda, Y.; Fujii, T.; Matsuo, M. Studies on Neurokinin Antagonists. 4. Synthesis and Structure–Activity Relationships of Novel Dipeptide Substance P Antagonists: N²-[(4*R*)-4-Hydroxyl-1-[(1-methyl-1*H*-indol-3-yl)carbonyl]-prolyl]-N-methyl-N-(phenylmethyl)-3-(2-naphthyl)-L-alaninamide and Its Related Compounds. *J. Med. Chem.* **1994**, *37*, 2090–2099.
- (22) Regoli, D.; Boudon, A.; Fauchère, J.-L. Receptors and Antagonists for Substance P and Related Peptides. *Pharmacol. Rev.* **1994**, *46*, 551–599.
- (23) Stevenson, G. I.; MacLeod, A. M.; Huscroft, I.; Cascieri, M. A.; Sadowski, S.; Baker, R. 4,4-Disubstituted Piperidines: A New Class of NK₁ Antagonist. *J. Med. Chem.* **1995**, *38*, 1264–1266.
- (24) Swain, C. J.; Fong, T. M.; Haworth, K.; Owen, S. N.; Seward, E. M.; Strader, C. D. Quinuclidine-Based NK-1 Antagonists, the Role of the Benzhydryl. *Bioorg. Med. Chem. Lett.* **1995**, *5*, 1261–1264.
- (25) Strader, C. D.; Fong, T. M.; Graziano, M. P.; Tota, M. R. The Family of G-Protein-Coupled Receptors. *FASEB J.* **1995**, *9*, 745–754.
- (26) Dammkoehler, R. A.; Karasek, S. F.; Shands, E. F. B.; Marshall, G. R. Constrained Search of Conformational Hyperspace. *J. Comput.-Aided Mol. Des.* **1989**, *3*, 3–21.
- (27) Beusen, D. D.; Shands, E. F. B. Systematic Search Strategies in Conformational Analysis. *Drug Discovery Today* **1996**, *1*, 429–437.
- (28) Cramer, R. D., III; Patterson, D. E.; Bunce, J. D. Comparative Molecular Field Analysis (CoMFA). 1. Effect of Shape on Binding of Steroids to Carrier Proteins. *J. Am. Chem. Soc.* **1988**, *110*, 5959–5967.
- (29) DePriest, S. A.; Mayer, D.; Naylor, C. B.; Marshall, G. R. 3D-QSAR of Angiotensin-Converting Enzyme and Thermolysin Inhibitors: A Comparison of CoMFA Models Based on Deduced and Experimentally Determined Active Site Geometries. *J. Am. Chem. Soc.* **1993**, *115*, 5372–5384.
- (30) Prendergast, K.; Adams, K.; Greenlee, W. J.; Nachbar, R. B.; Patchett, A. A.; Underwood, D. J. Derivation of a 3D Pharmacophore Model for the Angiotensin-II Site One Receptor. *J. Comput.-Aided Mol. Des.* **1994**, *8*, 491–512.
- (31) Fong, T. M.; Yu, H.; Cascieri, M. A.; Underwood, D.; Swain, C. J.; Strader, C. D. The Role of Histidine 265 in Antagonist Binding to the Neurokinin-1 Receptor. *J. Biol. Chem.* **1994**, *269*, 2728–2732.
- (32) Lowe, J. A., III; Ewing, F. E.; Snider, R. M.; Longo, K. P.; Constantine, J. W.; Lebel, W. S.; Woody, H. A.; Bordner, J. 2-Aryl-1-azabicyclo[2.2.2]octanes as Novel Nonpeptide Substance P Antagonists. *Bioorg. Med. Chem. Lett.* **1994**, *4*, 839–842.
- (33) Williams, B. J.; Teall, M.; McKenna, J.; Harrison, T.; Swain, C. J.; Cascieri, M. A.; Sadowski, S.; Strader, C.; Baker, R. Acyclic NK-1 Antagonists: 2-Benzhydryl-2-Aminoethyl Ethers. *Bioorg. Med. Chem. Lett.* **1994**, *4*, 1903–1908.
- (34) Seward, E. M.; Owen, S.; Sabin, V.; Swain, C. J.; Cascieri, M. A.; Sadowski, S.; Strader, C.; Baker, R. Quinuclidine-Based NK-1 Antagonists I: 3-Benzoyloxy-1-Azabicyclo[2.2.2]octanes. *Bioorg. Med. Chem. Lett.* **1993**, *3*, 1361–1366.
- (35) MacLeod, A. M.; Merchant, K. J.; Brookfield, F.; Kelleher, F.; Stevenson, G.; Owens, A. P.; Swain, C. J.; Cascieri, M. A.; Sadowski, S.; Ber, E.; Strader, C. D.; MacIntyre, D. E.; Metzger, J. M.; Ball, R. G.; Baker, R. Identification of L-Tryptophan Derivatives with Potent and Selective Antagonist Activity at the NK₁ Receptor. *J. Med. Chem.* **1994**, *37*, 1269–1274.
- (36) Lowe, J. A., III; Drozda, S. E.; McLean, S.; Crawford, R. T.; Bryce, D. K.; Bordner, J. N-Alkyl Quinuclidinium Substance P Antagonists. *Bioorg. Med. Chem. Lett.* **1994**, *4*, 1153–1156.
- (37) Lewis, R. T.; Macleod, A. M.; Merchant, K. J.; Kelleher, F.; Sanderson, I.; Herbert, R. H.; Cascieri, M. A.; Sadowski, S.; Ball, R. G.; Hoogsteen, K. Tryptophan-Derived NK₁ Antagonists: Conformationally Constrained Heterocyclic Bioisosteres of the Ester Linkage. *J. Med. Chem.* **1995**, *38*, 923–933.
- (38) Desai, M. C.; Vincent, L. A.; Rizzi, J. P. Importance of Parallel Vectors and “Hydrophobic Collapse” of the Aligned Aromatic Rings: Discovery of a Potent Substance P Antagonist. *J. Med. Chem.* **1994**, *37*, 4263–4266.
- (39) Natsugari, H.; Ikeura, Y.; Kiyota, Y.; Ishichi, Y.; Ishimaru, T.; Saga, O.; Shirafuji, H.; Tanaka, T.; Kamo, I.; Doi, T.; Otsuka, M. Novel, Potent, and Orally Active Substance P Antagonists: Synthesis and Antagonist Activity of N-Benzylcarboxamide Derivatives of Pyrido(3,4-*b*)pyridine. *J. Med. Chem.* **1995**, *38*, 3106–3120.
- (40) Ladduwahetty, T.; Baker, R.; Cascieri, M. A.; Chambers, M. S.; Haworth, K.; Keown, L. E.; MacIntyre, D. E.; Metzger, J. M.; Owen, S.; Rycroft, W.; Sadowski, S.; Seward, E. M.; Shephard, S. L.; Swain, C. J.; Tattersall, F. D.; Watt, A. P.; Williamson, D. W.; Hargreaves, R. J. N-Heteroaryl-2-phenyl-3-(benzyloxy) piperidines: A Novel Class of Potent Orally Active Human NK₁ Antagonists. *J. Med. Chem.* **1996**, *39*, 2907–2914.
- (41) Cascieri, M. A.; Macleod, A. M.; Underwood, D.; Shiao, L. L.; Ber, E.; Sadowski, S.; Yu, H.; Merchant, K. J.; Swain, C. J.; Strader, C. D.; Fong, T. M. Characterization of the Interaction of N-Acyl-L-Tryptophan Benzyl Ester Neurokinin Antagonists with the Human Neurokinin-1 Receptor. *J. Biol. Chem.* **1994**, *269*, 6587–6591.
- (42) Fong, T. M.; Yu, H.; Cascieri, M. A.; Underwood, D.; Swain, C. J.; Strader, C. D. Interaction of Glutamine 165 in the Fourth Transmembrane Segment of the Human Neurokinin-1 Receptor with Quinuclidine Antagonists. *J. Biol. Chem.* **1994**, *269*, 14957–14961.
- (43) MacLeod, A. M.; Cascieri, M. A.; Merchant, K. J.; Sadowski, S.; Hardwicke, S.; Lewis, R. T.; MacIntyre, D. E.; Metzger, J. M.; Fong, T. M.; Shephard, S.; Tattersall, F. D.; Hargreaves, R.; Baker, R. Synthesis and Biological Evaluation of NK₁ Antagonists Derived from L-Tryptophan. *J. Med. Chem.* **1995**, *38*, 934–941.
- (44) Desai, M. C.; Lefkowitz, S. L.; Bryce, D. K.; McLean, S. Articulating a Pharmacophore Driven Synthetic Strategy: Discovery of a Potent Substance P Antagonist. *Bioorg. Med. Chem. Lett.* **1994**, *4*, 1865–1868.
- (45) Oury-Donat, F.; Lefevre, I. A.; Gautier, T.; Edmonds-Alt, X.; LeFur, G.; Soubrie, P. SR 140333, A Novel and Potent Nonpeptide Antagonist of the NK₁ Receptor. *Neuropeptides* **1993**, *24*, 233.
- (46) Fong, T. M.; Cascieri, M. A.; Yu, Y.; Bansal, A.; Swain, C.; Strader, C. D. Amino-Aromatic Interaction between Histidine 197 of the Neurokinin-1 Receptor and CP 96,345. *Nature* **1993**, *362*, 350–353.
- (47) Lowe, J. A., III; Drozda, S. E.; McLean, S.; Bryce, D. K.; Crawford, R. T.; Snider, R. M.; Longo, K. P.; Nagahisa, A.; Tsuchiya, M. Aza-Tricyclic Substance P Antagonists. *J. Med. Chem.* **1994**, *37*, 2831–2840.
- (48) Strader, C. D. The View from Inside the Receptor. *J. Med. Chem.* **1996**, *39*, 1.
- (49) Takeuchi, Y.; Nonaka, T.; Nakamura, K. T.; Kojima, S.; Miura, K.; Mitsui, Y. Crystal Structure of an Engineered Subtilisin Inhibitor Complexed with Bovine Trypsin. *Proc. Natl. Acad. Sci. U.S.A.* **1992**, *89*, 4407–4411.
- (50) Takeuchi, Y.; Noguchi, S.; Satow, Y.; Kojima, S.; Kumagai, I.; Miura, K.; Nakamura, K. T.; Mitsui, Y. Molecular Recognition at the Active Site of Subtilisin BPN': Crystallographic Studies Using Genetically Engineered Proteinaceous Inhibitor SSI (Streptomyces Subtilisin Inhibitor). *Protein Eng.* **1991**, *4*, 501–508.
- (51) Sachais, B. S.; Snider, R. M.; Lowe, J. A.; Krause, J. E. Molecular Basis for the Species Selectivity of the Substance P Antagonist CP-96,345. *J. Biol. Chem.* **1993**, *268*, 2319–2323.
- (52) Jensen, C. J.; Gerard, N. P.; Schwartz, T. W.; Gether, U. The Species Selectivity of Chemically Distinct Tachykinin Nonpeptide Antagonists is Dependent on Common Divergent Residues of the Rat and Human Neurokinin-1 Receptors. *Mol. Pharmacol.* **1994**, *45*, 294–299.
- (53) SYBYL 6.1; Tripos, Inc., 1699 S. Hanley, St. Louis, MO 63144.
- (54) MM3 1.0; Tripos, Inc., 1699 S. Hanley, St. Louis, MO 63144.
- (55) RECEPTOR 3.2; Tripos, Inc., 1699 S. Hanley, St. Louis, MO 63144.
- (56) Clark, M.; Cramer, R., III; Van Opdenbosch, N. Validation of the General Purpose Tripos 5.2 Force Field. *J. Comput. Chem.* **1989**, *10*, 982–1012.
- (57) MOPAC 6.0; Quantum Chemistry Program Exchange.
- (58) Dewar, M. J. S.; Zoebish, E. G.; Healy, E. F.; Stewart, J. J. P. AM1: A New General Purpose Quantum Mechanical Molecular Model. *J. Am. Chem. Soc.* **1985**, *107*, 3902–3909.

- (59) Pradier, L.; Habertortoli, E.; Emile, L.; Leguern, J.; Loquet, I.; Bock, M. D.; Clot, J.; Mercken, L.; Fardin, V.; Garret, C.; Mayaux, J. F. Molecular Determinants Of the Species Selectivity Of Neurokinin Type 1 Receptor Antagonists. *Mol. Pharmacol.* **1995**, *47*, 314–321.
- (60) Stahle, L.; Wold, S. Partial Least Squares Analysis with Cross-validation for the Two-class Problem: a Monte Carlo Study. *J. Chemom.* **1987**, *1*, 185–196.
- (61) Cambridge Structural Database System 3; Cambridge Crystallographic Data Center, 12 Union Road, Cambridge CB2 1EZ, United Kingdom.
- (62) Cramer, R. D. I.; Bunce, J. D.; Patterson, D. E.; Frank, I. E. Crossvalidation, Bootstrapping, and Partial Least Squares Compared with Multiple Regression in Conventional QSAR Studies. *Quant. Struct.-Act. Relat.* **1988**, *7*, 18–25.
- (63) Cheng, Y.-C.; Prusoff, W. H. Relationship between the Inhibition Constant (K_i) and the Concentration of Inhibitor which Causes 50% Inhibition (I₅₀) of an Enzymatic Reaction. *Biochem. Pharmacol.* **1973**, *22*, 3099–3108.
- (64) Swain, C. J.; Seward, E. M.; Sabin, V.; Owen, S.; Baker, R.; Cascieri, M. A.; Sadowski, S.; Strader, C.; Ball, R. G. Quinuclidine Based NK-1 Antagonists 2: Determination of the Absolute Stereochemical Requirements. *Bioorg. Med. Chem. Lett.* **1993**, *3*, 1703–1706.
- (65) Harrison, T.; Owens, A. P.; Williams, B. J.; Swain, C. J.; Baker, R.; Hutson, P. H.; Sadowski, S.; Cascieri, M. A. Piperidine-Ether Based hNK₁ Antagonists 2: Investigation of the Effect of N-Substitution. *Bioorg. Med. Chem. Lett.* **1995**, *5*, 209–212.
- (66) Harrison, T.; Williams, B. J.; Swain, C. J. Gem-Disubstituted Amino-Ether Based Substance P Antagonists. *Bioorg. Med. Chem. Lett.* **1994**, *4*, 2733–2734.
- (67) Howard, H. R.; Shenk, K. D.; Coffman, K. C.; Bryce, D. K.; Crawford, R. T.; McLean, S. A. Synthesis of Conformationally Restricted Substance P Antagonists. *Bioorg. Med. Chem. Lett.* **1995**, *5*, 111–114.
- (68) Ofner, S.; Hauser, K.; Schilling, W.; Vassout, A.; Veenstra, S. J. SAR Of 2-Benzyl-4-Aminopiperidines: CGP 49823, An Orally And Centrally Active Non-Peptide NK₁ Antagonist. *Bioorg. Med. Chem. Lett.* **1996**, *6*, 1623–1628.
- (69) Veenstra, S. J.; Hauser, K.; Betschart, C. Studies On The Active Conformation Of NK₁ Antagonist CGP 49823. Part 1. Synthesis Of Conformationally Restricted Analogues. *Bioorg. Med. Chem. Lett.* **1997**, *7*, 347–350.
- (70) Veenstra, S. J.; Hauser, K.; Schilling, W.; Betschart, C.; Ofner, S. SAR Of 2-Benzyl-4-Aminopiperidines NK₁ Antagonists. Part 1. Synthesis of CGP 49823. *Bioorg. Med. Chem. Lett.* **1996**, *6*, 3029–3034.
- (71) Cascieri, M. A.; Shiao, L. L.; Mills, S. G.; Maccoss, M.; Swain, C. J.; Yu, H.; Ber, E.; Sadowski, S.; Wu, M. T.; Strader, C. D.; Fong, T. M. Characterization of the Interaction of Diacylpiperazine Antagonists with the Human Neurokinin-1 Receptor: Identification of a Common Binding Site for Structurally Dissimilar Antagonists. *Mol. Pharmacol.* **1995**, *47*, 660–665.
- (72) Swain, C. J.; Cascieri, M. A.; Owens, A.; Saari, W.; Sadowski, S.; Strader, C.; Teall, M.; VanNiel, M. B.; Williams, B. J. Acyclic NK₁ Antagonists: Replacements for the Benzhydryl Group. *Bioorg. Med. Chem. Lett.* **1994**, *4*, 2161–2164.

JM9700171